The Plant Cell, Vol. 19: 2662–2673, August 2007, www.plantcell.org

UV-B Promotes Rapid Nuclear Translocation of the *Arabidopsis* UV-B–Specific Signaling Component UVR8 and Activates Its Function in the Nucleus

Eirini Kaiserli and Gareth I. Jenkins[1]

Plant Science Group, Division of Biochemistry and Molecular Biology, Institute of Biomedical and Life Sciences, University of Glasgow, Glasgow G12 8QQ, United Kingdom

***Arabidopsis thaliana* UV RESISTANCE LOCUS8 (UVR8) is a UV-B–specific signaling component that binds to chromatin and regulates UV protection by orchestrating expression of a range of genes. Here, we studied how UV-B regulates UVR8. We show that UV-B stimulates the nuclear accumulation of both a green fluorescent protein (GFP)-UVR8 fusion and native UVR8. Nuclear accumulation leads to UV-B induction of the *HY5* gene, encoding a key transcriptional effector of the UVR8 pathway. Nuclear accumulation of UVR8 is specific to UV-B, occurs at low fluence rates, and is observed within 5 min of UV-B exposure. Attachment of a nuclear export signal (NES) to GFP-UVR8 causes cytosolic localization in the absence of UV-B. However, UV-B promotes rapid nuclear accumulation of NES-GFP-UVR8, indicating a concerted mechanism for nuclear translocation. UVR8 lacking the N-terminal 23 amino acids is impaired in nuclear translocation. Attachment of a nuclear localization signal (NLS) to UVR8 causes constitutive nuclear localization. However, NLS-GFP-UVR8 only confers *HY5* gene expression following UV-B illumination, indicating that nuclear localization, although necessary for UVR8 function, is insufficient to cause expression of target genes; UV-B is additionally required to stimulate UVR8 function in the nucleus. These findings provide new insights into the mechanisms through which UV-B regulates gene expression in plants.**

INTRODUCTION

UV-B wavelengths (280 to 320 nm) are a relatively minor component of sunlight but have a substantial impact on the biosphere because of their high energy (Caldwell et al., 1998, 2007). UV-B is potentially harmful to all organisms and is known to cause macromolecular damage and to inhibit cellular processes. For instance, in plants, UV-B has been reported to damage DNA and to generate reactive oxygen species, to inhibit photosynthetic reactions, and in some cases to cause necrosis (Dai et al., 1997; Jansen et al., 1998; Brosché and Strid, 2003; Jenkins and Brown, 2007). However, UV-B is not solely an agent of damage. It also acts as an informational signal that regulates UV-protective responses and developmental processes (Jansen et al., 1998; Frohnmeyer and Staiger, 2003; Paul and Gwynn-Jones, 2003; Ulm and Nagy, 2005; Jenkins and Brown, 2007). It is well established that many of the effects of UV-B entail the regulation of expression of a wide range of genes (Izaguirre et al., 2003; Casati and Walbot, 2004; Ulm et al., 2004; Brown et al., 2005; Casati et al., 2006). Therefore, it is important to understand the mechanisms of UV-B perception and signal transduction in plants and to establish how these processes lead to the regulation of gene expression.

[1] Address correspondence to g.jenkins@bio.gla.ac.uk.
The author responsible for distribution of materials integral to the findings presented in this article in accordance with the policy described in the Instructions for Authors (www.plantcell.org) is: Gareth I. Jenkins (g.jenkins@bio.gla.ac.uk).
www.plantcell.org/cgi/doi/10.1105/tpc.107.053330

The effects of UV-B wavelengths vary with the fluence rate of exposure. Damage may be caused by exposure to relatively high fluence rates of UV-B (Dai et al., 1997; Kim et al., 1998). The effect on the plant will be determined not only by the amount of UV-B but also by the wavelength (Ulm et al., 2004; Shinkle et al., 2004, 2005), the degree of prior acclimation, and to some extent by interaction with other environmental factors (Caldwell et al., 2007). High fluence rates of UV-B are known to generate reactive oxygen species (Dai et al., 1997; Allan and Fluhr, 1997; Barta et al., 2004) and to increase levels of signaling molecules involved in wound and defense responses, such as jasmonic acid and ethylene (A-H-Mackerness et al., 1999). It is therefore not surprising that UV-B stimulates expression of a number of genes characteristic of stress, defense, and wound responses. Thus, at high fluence rates, UV-B co-opts the perception and signaling mechanisms involved in stress, wound, and defense responses (A-H-Mackerness et al., 1999, 2001; Stratmann, 2003). The signaling pathways and target genes involved in these high fluence UV-B responses are therefore not UV-B specific.

In marked contrast with the potentially damaging effects of UV-B, low fluence rates of UV-B act as a regulatory, photomorphogenic signal that serves to protect plants against UV damage (Frohnmeyer and Staiger, 2003; Ulm and Nagy, 2005; Jenkins and Brown, 2007). Signs of UV damage are rarely seen in plants growing in the natural environment, demonstrating that UV protection is very effective. It is well known that UV-B stimulates the synthesis of flavonoids that act in conjunction with other phenolic compounds to provide a UV-absorbing sunscreen in epidermal tissues (Hahlbrock and Scheel, 1989; Li et al., 1993; Stapleton and Walbot, 1994; Bornman et al., 1997). The stimulation of

flavonoid accumulation is due to increased transcription of various genes encoding flavonoid biosynthesis enzymes in response to UV-B (Hahlbrock and Scheel, 1989; Weisshaar and Jenkins, 1998; Jenkins et al., 2001). In addition, low fluence rates of UV-B stimulate a range of other genes, including those involved in amelioration of oxidative stress and the repair of damaged DNA (Ulm et al., 2004; Brown et al., 2005). Photomorphogenic UV-B signals also regulate extension growth, expansion, and phototropic responses (Ballaré et al., 1995; Jansen et al., 1998; Kim et al., 1998; Boccalandro et al., 2001; Shinkle et al., 2004; 2005).

A number of studies have shown that signal transduction for responses to low fluence rate UV-B does not involve co-option of stress, wound, and defense signaling pathways (Jenkins et al., 2001; Jenkins and Brown, 2007). Furthermore, responses to UV-B above ~290 nm do not appear to be mediated either by DNA damage signaling, which may be involved in responses to shorter wavelengths, or by the known plant regulatory photoreceptors (Boccalandro et al., 2001; Wade et al., 2001; Brosché and Strid, 2003; Ulm et al., 2004; Jenkins and Brown, 2007). Action spectra show that wavelengths between 295 and 305 nm are most effective in low fluence UV-B responses (Ensminger, 1993), but a UV-B–specific photoreceptor has not been identified.

Recently, we demonstrated that the *Arabidopsis thaliana* UV RESISTANCE LOCUS8 (UVR8) protein acts as a UV-B–specific signaling component (Brown et al., 2005). The *uvr8* mutant was first identified in a screen for UV-sensitive plants (Kliebenstein et al., 2002) and was found to have reduced levels of flavonoids. The mutant fails to induce expression of the *CHALCONE SYNTHASE* gene in response to UV-B but retains induction in response to several other stimuli (Brown et al., 2005). Microarray studies demonstrated that UVR8 regulates a range of genes with important roles in UV protection and the repair of UV damage (Brown et al., 2005), explaining the sensitivity of the *uvr8* mutant to UV-B. Among the genes regulated by UVR8 are those encoding the HY5 and HYH transcription factors. These factors act redundantly to control expression of probably all the UVR8 target genes (B.A. Brown and G.I. Jenkins, unpublished data). HY5 in particular plays a key role in UV protection, and the *hy5* mutant is very sensitive to UV-B (Brown et al., 2005; Oravecz et al., 2006).

UVR8 has sequence similarity and putative structural similarity to the human RCC1 protein that regulates the small GTP binding protein Ran by catalyzing guanine nucleotide exchange (Kliebenstein et al., 2002). However, UVR8 has very little exchange activity and therefore has a different function to RCC1 (Brown et al., 2005). UVR8 associates strongly with chromatin via histones, and chromatin immunoprecipitation assays show that UVR8 binds to the *HY5* promoter region, indicating a direct involvement in mediating transcriptional regulation of the *HY5* gene (Brown et al., 2005). Our working hypothesis is that UVR8 facilitates the interaction of transcription factors that regulate the UV-B response with the *HY5* promoter.

Previous studies with transgenic plants expressing UVR8 fused to green fluorescent protein (GFP) indicated that UVR8 is localized in the cytoplasm as well as the nucleus (Brown et al., 2005). Here, we examine UVR8 localization in more detail in relation to function. We show that UV-B promotes rapid accumulation of UVR8 in the nucleus and provide evidence that this occurs via nuclear translocation. Nuclear localization is essential for function because of the chromatin association of UVR8. However, we found that nuclear localization is not sufficient for UVR8 activity and that UV-B is required to promote UVR8 function in the nucleus.

RESULTS

The Abundance of UVR8 Is Unaffected by Different Light Qualities

UV-B stimulates expression of a range of genes via the UVR8 pathway. We therefore wanted to investigate how UV-B regulates UVR8; possibilities included alteration of the amount, localization, or posttranslational modification of the protein. In the first instance, we examined whether UV-B affected the amount of UVR8 in leaf tissue. To monitor the abundance of the protein, we obtained antipeptide antibodies that specifically recognize UVR8. As shown in Figure 1A, when an antibody to a C-terminal region of the protein is used to probe a protein gel blot of *Arabidopsis* leaf proteins, a strong, specific signal is observed that is absent in the *uvr8-1* mutant. To examine the effects of light treatments on UVR8 abundance, plants grown in a low fluence rate of white light, equivalent to that used in previous gene expression studies (Brown et al., 2005), were exposed either to UV-B, UV-A, or red light or an increased fluence rate of white light. The amount of UVR8 was unaffected by any of these treatments (Figure 1A).

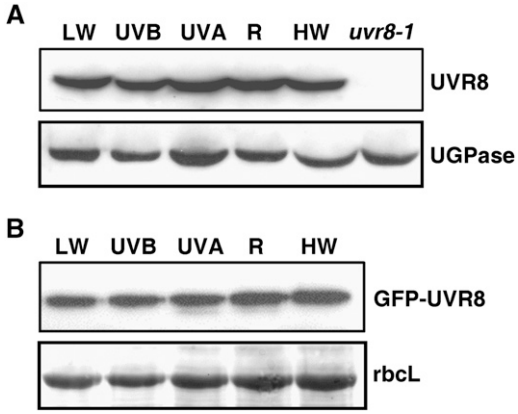

Figure 1. UVR8 and GFP-UVR8 Protein Levels Are Unaffected by Different Llight Qualities.

(A) Protein gel blot of total protein extracts from *Arabidopsis* Landsberg *erecta* (L*er*) and *uvr8-1* plants grown in 20 μmol m^{-2} s^{-1} white light (LW) and treated with either 3 μmol m^{-2} s^{-1} UV-B, 100 μmol m^{-2} s^{-1} UV-A, 100 μmol m^{-2} s^{-1} red (R), or 100 μmol m^{-2} s^{-1} white light (HW) for 4 h, probed with antibodies to UVR8 and to UGPase as a loading control.

(B) Protein gel blot of total proteins from transgenic *uvr8-1* plants expressing $UVR8_{pro}$*:GFP-UVR8* (line 6-2) grown and treated as in **(A)** probed with anti-GFP antibody. Ponceau staining of ribulose-1,5-bisphosphate carboxylase/oxygenase (Rubisco) large subunit (rbcL) is shown as a loading control.

UV-B Promotes Accumulation of UVR8 in the Nucleus

We wished to examine whether the intracellular distribution of UVR8 changed following UV-B illumination. In a previous study (Brown et al., 2005), we used plants expressing a GFP-UVR8 fusion protein driven by the cauliflower mosaic virus *35S* promoter to study UVR8 localization. To counter any potential problems with either the level or spatial distribution of expression from the heterologous *35S* promoter, we extended the experiments using the native *UVR8* promoter. As shown in Figure 2A, the *UVR8* promoter was effective in driving expression of GFP-UVR8 in transgenic *uvr8-1* null mutant plants. To establish that the fusion was functional, three independent lines were grown in white light lacking UV-B and then exposed to 4 h of UV-B at a fluence rate within the ambient range. This UV-B treatment induces expression of UV-protective genes via the UVR8 pathway (Brown et al., 2005). The GFP-UVR8 fusion is functional in that it complements the *uvr8* mutant; UV-B–induced expression of the *HY5* gene is impaired in the mutant but is restored in the transgenic lines (Figure 2B).

When plants grown in white light lacking UV-B are examined by confocal microscopy, the GFP-UVR8 fusion is detected in both the cytosol and nucleus, as can be seen in Figure 3A. However, UV-B exposure causes a marked increase in the number of nuclei displaying bright GFP-UVR8 fluorescence. By contrast, GFP alone, driven by the *35S* promoter, is not present in the nucleus and does not change its localization following UV-B exposure (Figure 3B).

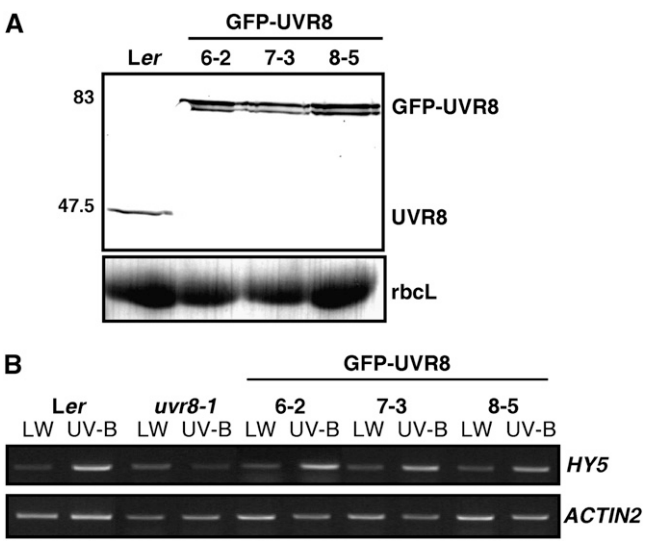

Figure 2. GFP-UVR8 Expressed from the *UVR8* Promoter Is Functional in Transgenic *uvr8-1* Mutant Plants.

(A) Protein gel blot of total protein extracts from L*er* and three independent lines of transgenic *uvr8-1* plants expressing *UVR8*$_{pro}$*:GFP-UVR8* probed with an anti-UVR8 antibody. Ponceau staining of Rubisco large subunit (rbcL) is shown as a loading control.

(B) RT-PCR assay of *HY5* and control *ACTIN2* transcripts in L*er*, *uvr8-1*, and *UVR8*$_{pro}$*:GFP-UVR8* lines grown in 20 μmol m^{-2} s^{-1} white light (LW) and exposed to 3 μmol m^{-2} s^{-1} UV-B for 4 h.

The change in localization of GFP-UVR8 is not accompanied by any alteration in abundance of the fusion protein. As shown in Figure 1B, exposure of the transgenic plants to various light treatments does not affect the amount of GFP-UVR8 detected on protein gel blots of leaf proteins by an anti-GFP antibody.

To quantify the change in GFP-UVR8 localization in response to UV-B, we used the fluorescent stain 4′,6-diamidino-2-phenylindole (DAPI) to identify nuclei in microscope images (Figure 3A) and then measured the percentage of those nuclei that also showed any detectable GFP fluorescence. The data in Figure 3C show that before UV-B treatment, ~40% of nuclei have detectable GFP fluorescence, whereas after UV-B exposure, the number rises to ~90%. Furthermore, we measured the brightness of GFP fluorescence in the nuclei. Following UV-B exposure, most of the nuclei have bright GFP fluorescence, whereas prior to UV-B treatment, a substantial proportion of the nuclei show dim GFP fluorescence (Figure 3D).

To establish whether UV-B promotes the accumulation of native UVR8 in the nucleus, we examined the abundance of the protein in cytosolic and nuclear fractions isolated from leaf tissue following UV-B exposure. Figure 4 shows that the fractions appear to be relatively free of cross-contamination, as judged by the lack of cross-reaction with antibodies to cytosolic and nuclear proteins, UDP-glucose pyrophosphorylase (UGPase) and histone H3, respectively. UVR8 is clearly more abundant in the cytosolic fraction than the nucleus, which is consistent with our calculation from confocal images that the volume of the cytosol is substantially greater than that of the nucleus in leaf epidermal cells. Following UV-B illumination, there is an increase in the amount of UVR8 detected in the nuclear protein fraction and a small decrease in the cytosolic fraction. The increase in UVR8 in the nuclear fraction is evidently not due to contamination from the cytosol.

The Nuclear Accumulation of UVR8 Is Specific to UV-B, Rapid, and Occurs at Low Fluence Rates

We wanted to examine whether the nuclear accumulation of UVR8 was specific to UV-B or occurred in response to other light qualities. Plants grown in white light lacking UV-B were exposed to either UV-B or to UV-A light to stimulate cryptochromes (Fuglevand et al., 1996) or to red light to promote formation of phytochrome Pfr. The nuclear localization of UVR8 was assayed by measuring GFP fluorescence relative to DAPI fluorescence, as described above (Figure 3C). The results (Figure 5A) demonstrate that nuclear accumulation of UVR8 is promoted only by UV-B.

Previous studies have shown that relatively brief exposure to UV-B is sufficient to induce changes in gene expression. In *Arabidopsis* cells, 5 min of UV-B is sufficient to stimulate a small increase in expression of the *CHS* gene, which is regulated by UVR8 (Jenkins et al., 2001). We therefore wished to establish whether a brief UV-B treatment could promote the nuclear accumulation of UVR8. As shown in Figure 5B, 30 min of UV-B illumination is sufficient to produce a maximal response, with ~90% of nuclei exhibiting GFP-UVR8 fluorescence, and as little as 10 min UV-B gives a clear increase in nuclear localization compared with the white light control. Interestingly, movement

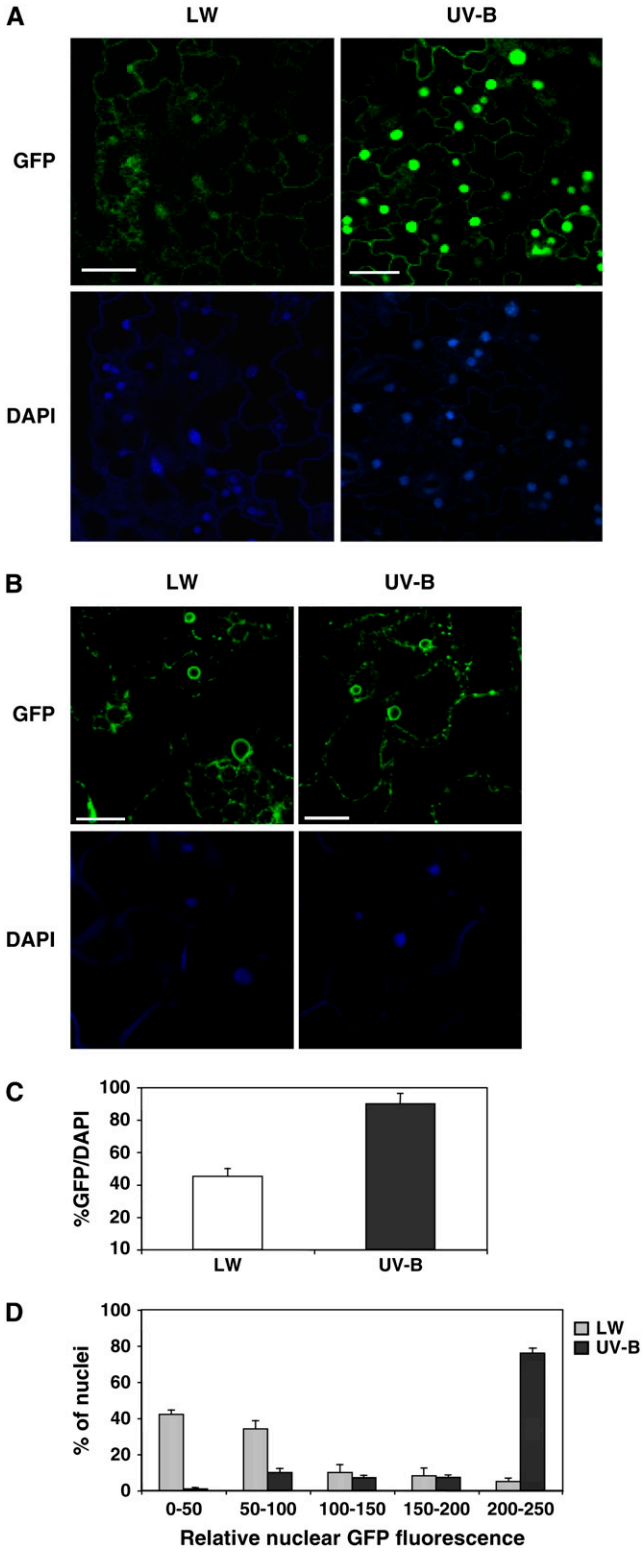

Figure 3. UV-B Stimulates Nuclear Accumulation of GFP-UVR8.

(A) Confocal images of GFP and DAPI fluorescence in leaf epidermal tissue of *UVR8*$_{pro}$*:GFP-UVR8* (line 6-2) plants grown in 20 μmol m^{-2} s^{-1} white light (LW) and exposed to 3 μmol m^{-2} s^{-1} UV-B for 4 h. Bars = 20 μm.

(B) Confocal images of GFP and DAPI fluorescence in leaf epidermal tissue of transgenic wild-type plants expressing GFP from the *35S* promoter grown in white light (LW) and exposed to UV-B as in **(A)**. Bars = 20 μm.

(C) The percentage of nuclei identified by DAPI fluorescence showing colocalization of GFP fluorescence before (LW) and after UV-B exposure as in **(A)**. Data are the mean ± SE (n = 20 images).

(D) Measurements of relative GFP-UVR8 fluorescence intensity of nuclei before (LW) and after UV-B illumination as in **(A)**. Data are the mean ± SE from three experiments each with at least 100 nuclei per treatment.

out of the nucleus is much slower, at least in darkness; a substantial amount of GFP-UVR8 was still present in nuclei 24 h after the transfer of UV-B–treated plants to darkness (Figure 5B).

We have recently found that UVR8 mediates gene expression responses to low fluence rates of UV-B (B.A. Brown and G.I. Jenkins, unpublished data). As little as 0.1 μmol m^{-2} s^{-1} UV-B, ~1/40 of the level in full sunlight, is sufficient to initiate expression of genes concerned with UV protection, such as *HY5* and *CHS*. It was therefore important to determine whether low fluence rates of UV-B promote the nuclear accumulation of GFP-UVR8. The results (Figure 5C) demonstrate that a clear increase in nuclear localization is observed at 0.1 μmol m^{-2} s^{-1} UV-B and a maximal response occurs at 0.5 μmol m^{-2} s^{-1} UV-B.

Accumulation of UVR8 in the Nucleus Is Correlated with Activity

The results presented in Figure 5 indicate that the nuclear accumulation of UVR8 may have functional significance in the regulation of gene expression by UV-B. To further explore this possibility, we examined whether manipulation of the localization of UVR8 affected its function. We attached a nuclear export signal (NES) at the N terminus of GFP-UVR8 and expressed the fusion in *uvr8* mutant plants using the *UVR8* promoter. This signal consisted of a peptide derived from the mammalian PKI protein (Wen et al., 1995) that was found to confer cytosolic localization of the N-terminal domain of phytochrome B (Matsushita et al., 2003). Several independent transgenic lines were produced. As can be seen in Figure 6A, the amount of the fusion expressed in several of these lines was similar to that of the GFP-UVR8 fusion. In transgenic plants grown in white light lacking UV-B, the NES-GFP-UVR8 fusion protein accumulated in the cytosol and was excluded from the nucleus (arrow in Figure 6B). GFP fluorescence was detected in only 1 to 2% of nuclei (Figure 6C) in contrast with the 40% accumulation seen in plants expressing GFP-UVR8 (Figure 3C). However, following UV-B illumination, the NES-GFP-UVR8 fusion accumulated in the nuclei to the same extent as the fusion lacking the NES (cf. Figures 6C and 3C). Moreover, accumulation occurred very rapidly (within 5 min) and at low fluence rates of UV-B, similar to the results with GFP-UVR8 (Figures 6C and 6D). The accumulation of the NES-GFP-UVR8 fusion in the nucleus following UV-B illumination resulted in complementation of the mutant phenotype with respect to expression of the *HY5* gene, which encodes a key transcriptional target of UVR8 (Figure 6E). Similar results were found with other genes, such as *CHS* (data not shown).

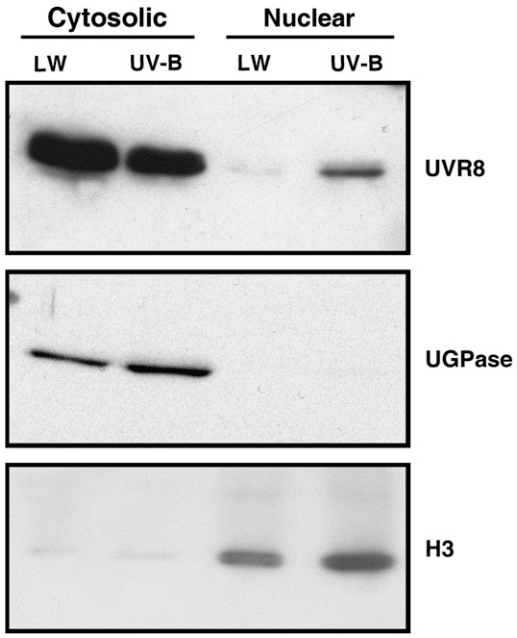

Figure 4. UV-B Stimulates Nuclear Accumulation of Native UVR8.

Protein gel blot of cytosolic and nuclear fractions (20 and 30 μg protein, respectively) of L*er* plants grown in 20 μmol m^{-2} s^{-1} white light (LW) and treated with 3 μmol m^{-2} s^{-1} UV-B for 4 h probed with anti-UVR8, anti-UGPase, and anti-histone H3 antibodies.

In a further attempt to prevent UVR8 accumulating in the nucleus, we produced transgenic *uvr8* plants expressing GFP fused to an N-terminal 23–amino acid deletion of UVR8 (GFP-ΔNUVR8). The human RCC1 protein, which shares ~50% sequence similarity with UVR8 (Kliebenstein et al., 2002), has a bipartite nuclear localization signal (NLS) toward the N terminus, and although the equivalent region of UVR8 does not have an obvious NLS, we reasoned that it might still be involved in nuclear import. Several transgenic lines were produced that expressed GFP-ΔNUVR8 (Figure 7A). Plants grown in white light lacking UV-B accumulated the GFP-ΔNUVR8 fusion in the cytosol and nucleus (Figure 7B), at similar levels to GFP-UVR8 (Figure 7C). However, following UV-B illumination, there was only a small increase in the proportion of nuclei showing GFP fluorescence, indicating that nuclear accumulation of GFP-ΔNUVR8 was substantially impaired. We did not observe UV-B stimulation of *HY5* expression following UV-B illumination in the GFP-ΔNUVR8 plants (Figure 7D) nor stimulation of *CHS* expression (data not shown). Nevertheless, a chromatin immunoprecipitation assay (Figure 7E) demonstrated that the GFP-ΔNUVR8 fusion was capable of binding to chromatin at the *HY5* promoter, similar to GFP-UVR8 (Brown et al., 2005), indicating that it had the potential to function in transcriptional regulation of the *HY5* gene.

UVR8 Function in the Nucleus Requires UV-B Illumination

We wanted to determine whether the presence of a cytoplasmic pool of UVR8 was required for the protein to be functional and, furthermore, whether constitutive localization of UVR8 in the nucleus was sufficient for its activity. To address these questions, we attached an NLS at the N terminus of GFP-UVR8 and expressed the fusion in *uvr8* mutant plants via the *UVR8* promoter. The NLS was a peptide from SV40 that has been shown to direct nuclear localization of the N-terminal region of phytochrome B (Matsushita et al., 2003). Several transgenic lines were produced, and the level of NLS-GFP-UVR8 was similar to that of GFP-UVR8, as shown in Figure 8A. Plants expressed NLS-GFP-UVR8

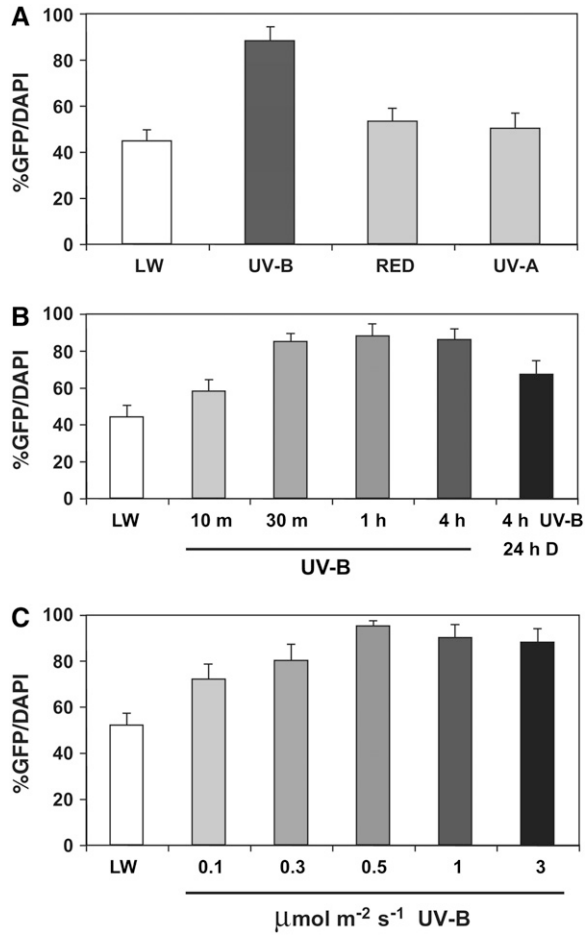

Figure 5. Spectral Specificity, Kinetics, and Fluence Rate Dependence of GFP-UVR8 Nuclear Accumulation.

(A) The percentage of nuclei identified by DAPI fluorescence showing colocalization of GFP fluorescence in $UVR8_{pro}$:*GFP-UVR8* (line 6-2) plants grown in 20 μmol m^{-2} s^{-1} white light (LW) and exposed to either 3 μmol m^{-2} s^{-1} UV-B, 100 μmol m^{-2} s^{-1} red, or 100 μmol m^{-2} s^{-1} UV-A light for 4 h.

(B) Nuclear GFP/DAPI colocalization in $UVR8_{pro}$:*GFP-UVR8* (line 6-2) plants grown in white light (LW) as in **(A)** and exposed to UV-B (3 μmol m^{-2} s^{-1}) for 10 min, 30 min, 1 h, 4 h, or 4 h then transferred to darkness (D) for 24 h.

(C) Nuclear GFP/DAPI colocalization in $UVR8_{pro}$:*GFP-UVR8* (line 6-2) plants grown in white light (LW) as in **(A)** and exposed to different fluence rates of UV-B (0.1, 0.3, 0.5, 1, and 3 μmol m^{-2} s^{-1}) for 4 h.

Data for all graphs are the mean ± SE ($n = 20$ images).

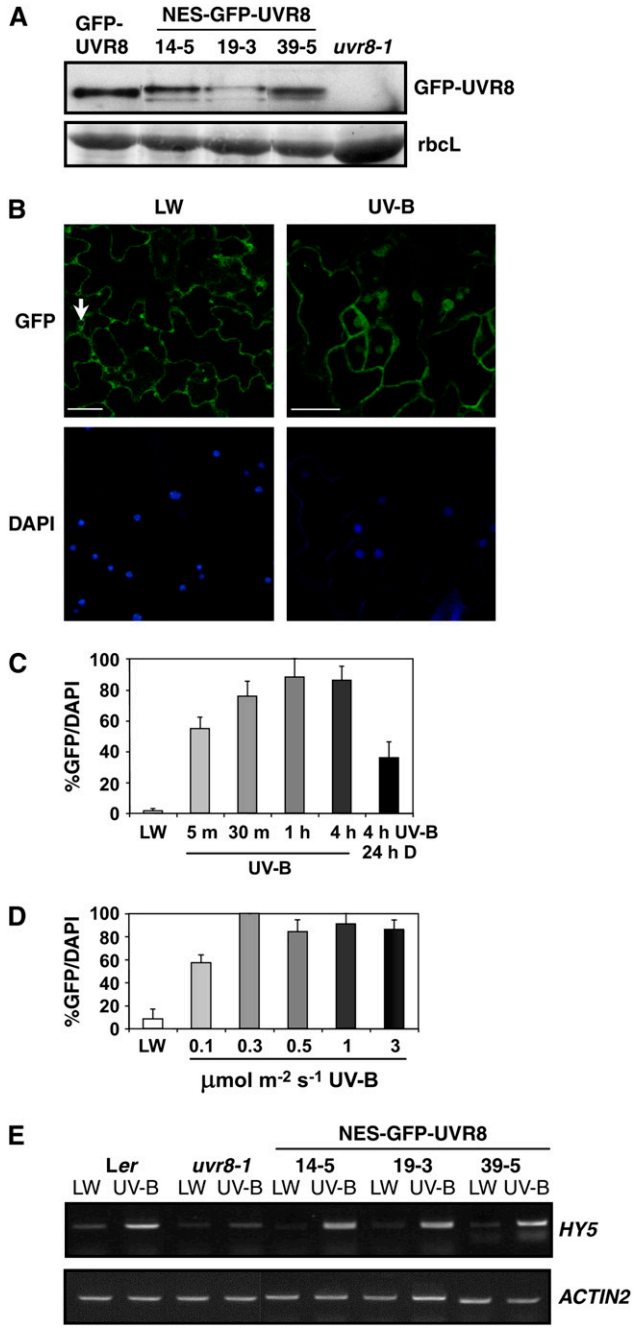

Figure 6. UV-B Induces Nuclear Accumulation of the NES-GFP-UVR8 Fusion.

(A) Protein gel blot of total protein extracts from *UVR8$_{pro}$:GFP-UVR8* plants (line 6-2), *uvr8-1*, and three independent lines of *uvr8-1* plants expressing NES-GFP-UVR8 from the *UVR8* promoter probed with an anti-GFP antibody. Ponceau staining of Rubisco large subunit (rbcL) is shown as a loading control.

(B) Confocal images of GFP and DAPI fluorescence in leaf epidermal tissue of *UVR8$_{pro}$:NES-GFP-UVR8* transgenic plants (line 14-5) grown in 20 μmol m^{-2} s^{-1} white light (LW) and exposed to 3 μmol m^{-2} s^{-1} UV-B for 4 h. The arrow indicates a nucleus with no GFP fluorescence. Bars = 20 μm.

(C) The percentage of nuclei identified by DAPI fluorescence showing colocalization of GFP fluorescence in *UVR8$_{pro}$:NES-GFP-UVR8* plants (line 14-5) grown in white light (LW) as in **(B)** and exposed to UV-B (3 μmol m^{-2} s^{-1}) for 5 min, 30 min, 1 h, 4 h, or 4 h then transferred to darkness for 24 h. Data are the mean ± SE (n = 20 images).

(D) Nuclear GFP/DAPI colocalization in *UVR8$_{pro}$:NES-GFP-UVR8* plants (line 14-5) grown in white light (LW) as in **(B)** and exposed to different fluence rates of UV-B (0.1, 0.3, 0.5, 1, and 3 μmol m^{-2} s^{-1}) for 4 h. Data are the mean ± SE (n = 20 images).

(E) RT-PCR assay of *HY5* and control *ACTIN2* transcripts in L*er*, *uvr8-1*, and *UVR8$_{pro}$:NES-GFP-UVR8* lines grown in white light (LW) and exposed to UV-B as in **(B)**.

constitutively in the nucleus regardless of the light conditions (Figure 8B). The amount of the protein in the nucleus showed little change over 24 h from the start of UV-B illumination (Figure 8C). However, the NLS-GFP-UVR8 plants only showed elevated *HY5* expression following UV-B illumination and not in white light lacking UV-B (Figure 8D).

DISCUSSION

UV-B Promotes Nuclear Accumulation of UVR8

In plants grown in white light lacking UV-B, GFP-UVR8 is localized in both the cytoplasm and nucleus. Although our studies have focused on leaf epidermal cells, the same distribution is observed in other tissues and organs (data not shown). Within the cytoplasm, localization appears to be principally cytosolic and not associated with any particular organelle or the plasma membrane. Two lines of evidence indicate that most of the UVR8 in the cell is in the cytoplasm. First, we estimate, from confocal images of epidermal cells, that the volume of the cytoplasm is ~10 times that of the nucleus and, taking into account the relative brightness of GFP fluorescence in the cytoplasm and nucleus, it is evident that most of the GFP-UVR8 is in the cytoplasm. The intensity of GFP-UVR8 fluorescence in the small volume of the nucleus gives an unrealistic impression of the relative amount in the nuclear fraction. Second, the immunological detection of native UVR8 in cellular fractions (Figure 4) indicates that most of the protein is cytoplasmic. Although both these analyses are qualitative rather than quantitative, they indicate that the nuclear pool of UVR8 is relatively small, which is perhaps surprising given that the protein functions in the nucleus.

Exposure to UV-B promotes the nuclear accumulation of both GFP-tagged and native UVR8. Measurement of the colocalization of GFP and DAPI in confocal images (Figure 3C) indicates that the number of nuclei containing GFP-UVR8 rises from 40 to 90% after UV-B treatment. However, this analysis underestimates the difference in amount of GFP-UVR8 in the nuclei before and after UV-B treatment because it does not take into account the change in intensity of GFP fluorescence in the nuclei. Before UV-B illumination, most of the nuclei containing GFP have dim fluorescence, whereas after UV-B, few nuclei are in this category and ~80% have bright fluorescence (Figure 3D). The protein gel blot analysis also indicates a strong increase in nuclear accumulation of UVR8 in response to UV-B, although the amount in the nucleus remains smaller than that in the cytoplasm.

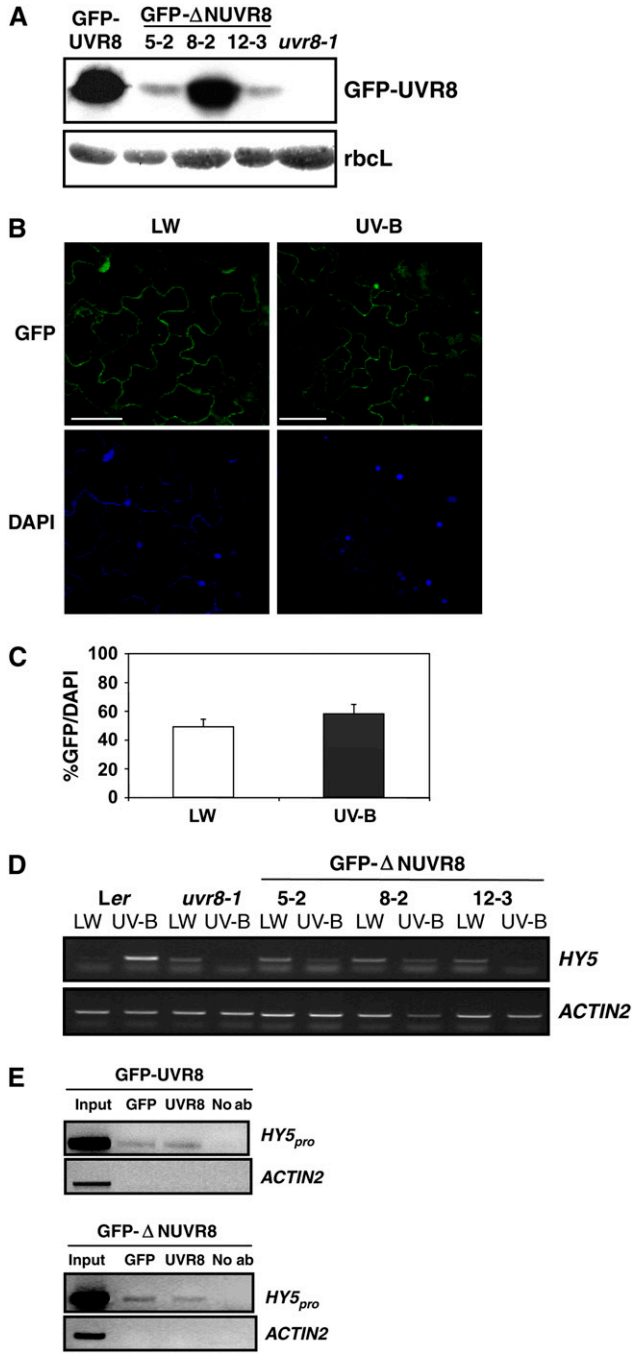

Figure 7. The GFP-ΔNUVR8 Fusion Protein Is Impaired in UV-B–Specific Nuclear Accumulation and Fails to Complement Transgenic *uvr8-1* Plants.

(A) Protein gel blot of total protein extracts from *UVR8*$_{pro}$*:GFP-UVR8* (line 6-2), *uvr8-1*, and three independent lines of *uvr8-1* plants expressing GFP-ΔNUVR8 from the *UVR8* promoter probed with an anti-GFP antibody. Ponceau staining of Rubisco large subunit (rbcL) is shown as a loading control.

(B) Confocal images of GFP and DAPI fluorescence in leaf epidermal tissue of *UVR8*$_{pro}$*:GFP-ΔNUVR8* plants (line 8-2) grown in 20 μmol m^{-2} s^{-1} white light (LW) and exposed to 3 μmol m^{-2} s^{-1} UV-B for 4 h. Bars = 20 μm.

(C) The percentage of nuclei identified by DAPI fluorescence showing colocalization of GFP fluorescence before (LW) and after UV-B exposure of *UVR8*$_{pro}$*:GFP-ΔNUVR8* (line 8-2) plants as in **(B)**. Data are the mean ± SE ($n = 20$ images).

(D) RT-PCR assay of *HY5* and control *ACTIN2* transcripts in L*er*, *uvr8-1*, and *UVR8*$_{pro}$*:GFP-ΔNUVR8* lines grown in white light (LW) and exposed to UV-B as in **(B)**.

(E) Chromatin immunoprecipitation assay of DNA associated with GFP-UVR8 or GFP-ΔNUVR8. PCR of *HY5* promoter (−331 to +23) and control *ACTIN2* DNA from *UVR8*$_{pro}$*:GFP-UVR8* (line 6-2) (top panel) and *UVR8*$_{pro}$*:GFP-ΔNUVR8* (line 8-2) (bottom panel) transgenic plants grown in white light and exposed to UV-B as in **(B)**. Lane 1, input DNA before immunoprecipitation; lane 2, DNA immunoprecipitated by anti-GFP antibody; lane 3, DNA immunoprecipitated by anti-UVR8 antibody; lane 4, no antibody control.

Evidence for a UV-B–Stimulated Nuclear Translocation Mechanism

The nuclear accumulation of UVR8 occurs without any change in the total amount of the protein. UV-B, and indeed other light qualities, do not affect the abundance of either the GFP-UVR8 fusion (Figure 1B) or the native protein (Figure 1A), consistent with *UVR8* transcript measurements (Kliebenstein et al., 2002). Hence, the simplest explanation of the nuclear accumulation of UVR8 is that UV-B promotes a redistribution of UVR8 within the cell by stimulating movement from the cytoplasm into the nucleus. An alternative possibility is that UVR8 continually cycles between the cytoplasm and nucleus and that UV-B inhibits translocation into the cytosol, thereby causing nuclear accumulation. However, such a mechanism is insufficient to explain all the data, in particular the results with the NES-GFP-UVR8 fusion. The NES-GFP-UVR8 fusion is excluded from the nucleus in white light lacking UV-B but accumulates in the nucleus following UV-B exposure (Figure 6C). An inhibition of nuclear export by UV-B does not explain these observations, and the most logical interpretation is that UV-B actively stimulates nuclear accumulation of the NES-GFP-UVR8 fusion.

Another possible explanation of the nuclear accumulation of UVR8 in response to UV-B is that UV-B does not promote movement, but instead both inhibits degradation of the nuclear pool and stimulates destruction of the cytosolic pool without affecting the net amount of the protein. Again, the results with the NES-GFP-UVR8 fusion do not support this possibility because there does not appear to be a nuclear pool of NES-GFP-UVR8 prior to UV-B illumination; therefore, inhibition of its degradation could not lead to accumulation. One could argue that the NES does not prevent nuclear import in the absence of UV-B, and its presence leads to complete destruction of nuclear NES-GFP-UVR8, which is then prevented following UV-B illumination. However, such a mechanism seems very unlikely. Experiments with the NLS-GFP-UVR8 fusion also do not support the idea of UV-B preventing nuclear destruction of UVR8. The fusion was clearly present in the nucleus prior to UV-B illumination (Figure 8C) and thus was not being destroyed. Moreover, there was no change in amount even 24 h after the start of UV-B illumination (Figure 8D), in contrast with the increase predicted by the inhibition of destruction model.

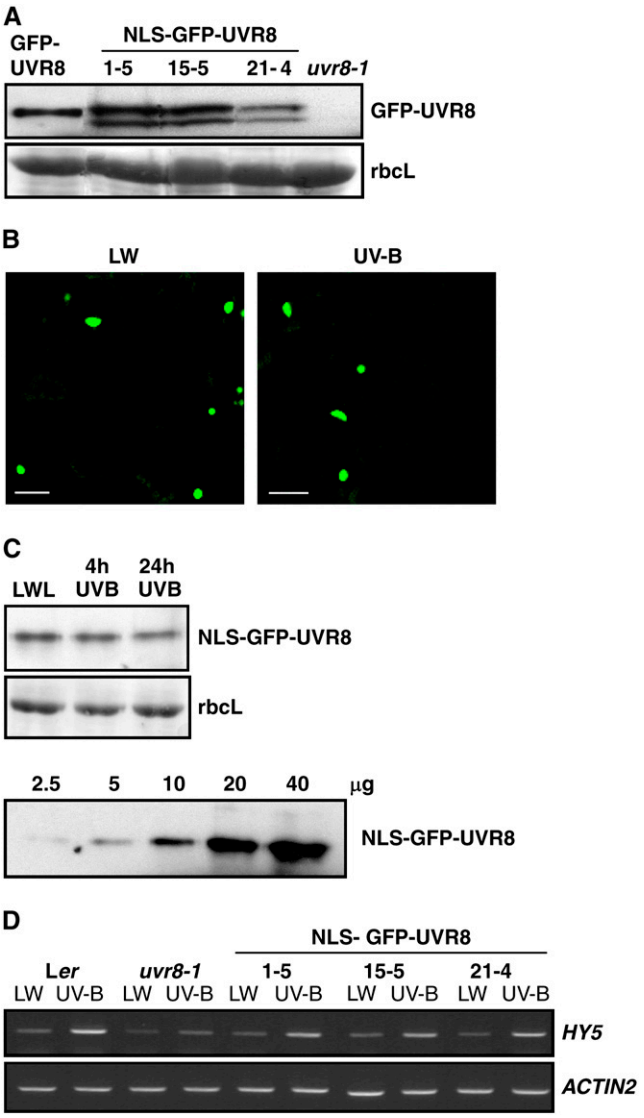

Figure 8. The NLS-GFP-UVR8 Fusion Protein Is Constitutively Nuclear but Requires UV-B for Function.

(A) Protein gel blot of total protein extracts from *UVR8*$_{pro}$*:GFP-UVR8* (line 6-2), *uvr8-1*, and three independent lines of *uvr8-1* plants expressing NLS-GFP-UVR8 from the *UVR8* promoter probed with an anti-GFP antibody. Ponceau staining of Rubisco large subunit (rbcL) is shown as a loading control.

(B) Confocal image of GFP fluorescence in leaf epidermal tissue of *UVR8*$_{pro}$*:NLS-GFP-UVR8* (line 1-5) plants grown in 20 μmol m^{-2} s^{-1} white light (LW) and exposed to 3 μmol m^{-2} s^{-1} UV-B for 4 h. Bars = 20 μm.

(C) Top panel: protein gel blot of total protein extracts (5 μg) from *UVR8*$_{pro}$*:NLS-GFP-UVR8* (line 1-5) plants grown in white light (LW) as in **(B)** and exposed to 3 μmol m^{-2} s^{-1} UV-B for 4 or 24 h probed with an anti-GFP antibody. Ponceau staining of Rubisco large subunit (rbcL) is shown as a loading control. Bottom panel: protein gel blot as above, showing increased amounts of protein (LW sample) loaded on the gel.

(D) RT-PCR assay of *HY5* and control *ACTIN2* transcripts in L*er*, *uvr8-1*, and *UVR8*$_{pro}$*:NLS-GFP-UVR8* lines grown in white light (LW) and exposed to UV-B as in **(B)**.

Thus, taken together, our data indicate that UV-B actively promotes translocation of a fraction of the cytoplasmic pool of UVR8 into the nucleus. This conclusion is consistent with the observed redistribution of GFP-UVR8 and native UVR8 in the absence of any net change in abundance of the protein. Furthermore, the observation that UV-B overcomes the ability of the NES to retain GFP-UVR8 in the cytoplasm points to a concerted mechanism for nuclear import of UVR8 in response to UV-B. As shown in Figure 5, this mechanism is specific to UV-B and able to drive rapid nuclear accumulation of GFP-UVR8. There is no precedent for such a mechanism in plant cells. Although there is recent evidence that COP1 accumulates in the nucleus in response to UV-B, the response is very slow and takes ~24 h (Oravecz et al., 2006). Quite rapid nuclear translocation of proteins in response to UV-B has been reported in mammalian cells, for instance, for the Nrf2 transcription factor (Kannan and Jaiswal, 2006) and Fyn protein kinase (He et al., 2005), but the mechanism is unknown. In plants, the most comparable response to that reported here is the rapid nuclear accumulation of phytochrome Pfr in response to red (phyB) or red and far-red wavelengths (phyA) (Kircher et al., 1999; Yamaguchi et al., 1999).

The UV-B–specific nuclear translocation mechanism could regulate the localization of additional proteins, but no information is available on this point. In addition, we have very little information on the mechanism of nuclear translocation. The data presented in Figure 7C indicate that the N-terminal 23 amino acids of UVR8 are required for efficient nuclear translocation, as deletion of this region reduces import by ~70%. There is no cluster of basic amino acids characteristic of a classic NLS in this region. Thus, we speculate that the N-terminal region binds proteins that facilitate nuclear import specifically in response to UV-B. Evidence that some proteins enter the nucleus by binding to other proteins containing an NLS has been obtained in experiments with mammalian cells (e.g., Dostie et al., 2000; Kong et al., 2000), and in plants, the nuclear accumulation of phyA is regulated through interaction with FHY1 and FHL (Hiltbrunner et al., 2006).

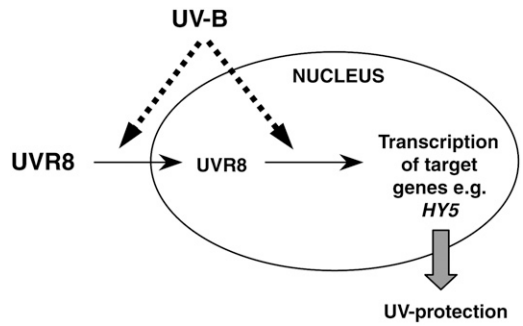

Figure 9. Model Showing the Dual Role of UV-B in Regulating UVR8.

UV-B stimulates both the nuclear translocation of a fraction of the cytoplasmic UVR8 pool (drawn larger than the nuclear pool) and the function of UVR8 in the nucleus, leading to increased transcription of genes, such as *HY5*, that confer UV protection.

Nuclear Accumulation of UVR8 Correlates with Function

UVR8 is required for the UV-B–induced expression of a set of genes concerned with UV protection (Brown et al., 2005). The data presented here show that the nuclear accumulation of UVR8 is directly related to its role in regulating gene expression. UVR8 nuclear accumulation is stimulated specifically by UV-B rather than other light qualities, consistent with its UV-B–specific function. In addition, the rapid accumulation of UVR8 in the nucleus correlates with previous observations that brief exposure to UV-B is sufficient to initiate expression of genes regulated by UVR8, such as *CHS* (Jenkins et al., 2001). Moreover, the nuclear accumulation of UVR8 occurs over the range of fluence rates that promote gene expression responses mediated by UVR8 (B.A. Brown and G.I. Jenkins, unpublished data). Experiments with the NES-GFP-UVR8 line show that significant nuclear accumulation occurs after 5 min of UV-B exposure and at a low fluence rate (Figures 6D and 6E). The NES-GFP-UVR8 line is evidently a very useful tool for further characterizing the nuclear translocation response because negligible accumulation is observed in the absence of UV-B.

The ability of GFP-UVR8 to complement the *uvr8* mutant phenotype allowed us to investigate directly the function of UVR8 in the regulation of gene expression. In these experiments, we monitored *HY5* transcript accumulation because UVR8 controls *HY5* expression specifically in UV-B and HY5 effects transcription of most, if not all, UVR8 regulated genes (Brown et al., 2005; B.A. Brown and G.I. Jenkins, unpublished data). HY5 is required for UV protection, and the *hy5* mutant is just as sensitive to UV-B as *uvr8* (Brown et al., 2005). Thus, by assaying *HY5* expression in the transgenic lines, we are able to relate UVR8 localization to plant UV protection.

Our previous report that GFP-UVR8 binds to chromatin in the region of genes it regulates (Brown et al., 2005) provides strong evidence that nuclear localization is required for UVR8 function. Thus, it would not be surprising if any treatment that impaired the nuclear accumulation of UVR8 resulted in a loss of function. Transgenic plants expressing GFP-ΔNUVR8 have impaired nuclear translocation of the fusion in response to UV-B and lack UV-B induction of *HY5* expression. Although the greatly reduced amount of GFP-ΔNUVR8 in the nucleus probably reduced the capacity for *HY5* expression, it may not account for the complete absence of *HY5* induction in response to UV-B. It is possible that the N-terminal region of UVR8 is required for its maximal activity as well as its efficient nuclear translocation. However, GFP-ΔNUVR8 retains the capacity to bind to chromatin at the *HY5* promoter (Figure 7E), indicating that it may be functional.

When UVR8 is constitutively localized in the nucleus using an NLS, it is able to direct *HY5* expression in response to UV-B illumination. Furthermore, the results with the NLS-GFP-UVR8 fusion show that the maintenance of a cytoplasmic pool of UVR8 is not essential for its function in stimulating transcription. So what is the purpose of the cytoplasmic pool and of nuclear translocation? A possible explanation is that the nuclear activity of UVR8 results in turnover of the protein and nuclear translocation is required to replenish the nuclear pool. Although the amount of NLS-GFP-UVR8 remains roughly constant over 24 h of UV-B illumination, turnover and replacement may still be occurring. Synthesis of the NLS-GFP-UVR8 fusion will continue during UV-B illumination, but the protein will be directly imported into the nucleus rather than accumulate in the cytoplasm. Thus, the cytoplasmic pool may simply serve as a buffer to regulate the level of nuclear import in relation to nuclear activity. Alternatively, it is possible that cytoplasmic UVR8 has an undiscovered function. Hence, further research is needed to examine turnover of the protein and function of the cytoplasmic pool.

UV-B Illumination Is Necessary for UVR8 Function in the Nucleus

Although the presence of UVR8 in the nucleus is required for its function, nuclear localization is not sufficient for function. The GFP-UVR8 fusion is present in the nucleus in white light lacking UV-B, but minimal *HY5* expression is observed (Figure 2A). Furthermore, the results in Figure 8D show that constitutive localization of the NLS-GFP-UVR8 fusion in the nucleus is insufficient to promote *HY5* expression in the absence of UV-B. We therefore conclude that UV-B illumination is required for the nuclear activity of UVR8. This may involve direct activation of UVR8 in some way or the activation of some other component that acts in the UVR8 pathway to stimulate transcription. The results with the NLS-GFP-UVR8 fusion show that the process of UVR8 nuclear import itself does not lead to UVR8 activation. Figure 9 summarizes our model of UVR8 action and regulation. It shows that UV-B illumination both stimulates the movement of a fraction of the cellular pool of UVR8 into the nucleus and is required for UVR8 function in the nucleus.

The site of UV-B perception in the above processes is uncertain. At present, there is no evidence from studies of the heterologously expressed protein that UVR8 itself acts as a UV-B photoreceptor. The experiments with the NLS-GFP-UVR8 fusion show that UV-B illumination is required for UVR8 function in the nucleus, but that does not necessarily mean that UV-B is detected in the nucleus. It is conceivable that cytoplasmic UV-B perception directs the rapid nuclear translocation of an unidentified component that is required for activation of the UVR8 pathway in the nucleus. However, it is not clear that nuclear translocation involves cytoplasmic UV-B perception because a signal could emanate from the nucleus as a result of UV-B photoreception that activates rapid nuclear translocation. Thus, the nature and site of UV-B photoreception remain a mystery.

METHODS

Plant Materials and Treatments

Seeds of wild-type *Arabidopsis thaliana* ecotype L*er* were obtained from the Nottingham Arabidopsis Stock Centre. The *uvr8-1* mutant allele in the L*er* background (Kliebenstein et al., 2002) was obtained from Dan Kliebenstein (University of California, Davis). All the transgenic lines were produced in the *uvr8-1* mutant.

For chromatin immunoprecipitation assays, subcellular localization analyses, and most of the protein studies, seeds were surface sterilized and sown on filter paper on 0.8% agar plates containing half-strength Murashige and Skoog (MS) salts. Plates were cold treated in the dark at 4°C for 48 h and plants grown for 12 d at 21°C under 20 μmol m^{-2} s^{-1}

constant white light (Osram warm white fluorescent tubes). Plants were given light treatments as described in the figure legends using light sources for UV-B, UV-A, or red light described by Wade et al. (2001). The UV-B source (UV-B-313 fluorescent tubes; Q-Panel) was covered with cellulose acetate, which was changed every 24 h. This source emits maximally at 313 nm and has no emission below 290 nm. It emits very low levels of UV-A and blue light that are insufficient to induce *CHS* expression (Christie and Jenkins, 1996). Fluence rates were measured either using a Skye RS232 meter (Skye Instruments) equipped with a Quantum sensor or SKU 430 sensor (280 to 315 nm) or using a Macam spectroradiometer (model SR9910; Macam Photometrics).

For RT-PCR analysis of transgenic lines, cellular fractionation experiments, and some of the protein studies, plants were grown on compost for 3 weeks under 20 μmol m^{-2} s^{-1} constant white light at 21°C and then treated with 3 μmol m^{-2} s^{-1} UV-B for 4 h.

Plasmid Constructs and Transformation

To generate gene fusions driven by the native *UVR8* promoter, the –1426 to +163 genomic sequence upstream of the *UVR8* coding sequence was PCR amplified using the following primers: forward, 5′-GTATATAG-TACTTCCAATGGC-3′; reverse, 5′-ATCACAGTTGCAGTTTTCACA-3′. This promoter fragment replaced the cauliflower mosaic virus *35S* promoter upstream of GFP in the pEZR(K)-LC vector (Brown et al., 2005) at restriction sites 5′ *Sac*I and 3′ *Hin*dIII. UVR8 and ΔNUVR8 (UVR8 lacking the first 23 amino acids) cDNA sequences were PCR amplified and cloned at restriction sites 5′ *Eco*RI and 3′ *Sal*I in the modified pEZR(K)-LC vector. The NLS and NES sequences used for the generation of NLS-GFP-UVR8 and NES-GFP-UVR8 constructs were PCR synthesized as described by Matsushita et al. (2003). DNA sequencing confirmed that each fusion had been made correctly.

The fusions were introduced into *uvr8-1* mutant plants by *Agrobacterium tumefaciens*–mediated transformation using the floral dip method (Bechtold and Pelletier, 1998). T1 seed from transformed plants was selected on 0.8% agar plates containing half-strength MS salts and 75 μg/mL of kanamycin. T2 generation plants exhibiting 3:1 segregation were selected.

At least four independent homozygous T3 lines were tested for protein expression, localization studies, and complementation of gene expression. Similar results were obtained from all lines expressing a particular fusion even though data are presented from only one line.

Protein Extraction and Protein Gel Blot Analysis

Total protein was extracted by grinding plants in microextraction buffer (20 mM HEPES, pH 7.8, 450 mM NaCl, 50 mM NaF, 200 μM EDTA, 500 μM PMSF, 1 mM DTT, and 25% glycerol with one protease inhibitor mix tablet [Complete Mini; Roche] added per 10 mL of buffer). Homogenization was followed by a freeze-thaw treatment (10 s on dry ice followed by 10 s at 37°C) repeated three times. The homogenate was centrifuged for 10 min at 16,100*g* in a microcentrifuge at 4°C, and the supernatant was collected. Nuclear and cytosolic fractions were obtained and used for protein extraction as described by Cho et al. (2006). The protein concentration of the total, nuclear, and cytosolic fractions was determined by a Bradford assay (Bio-Rad), and equal amounts of protein were loaded on a 10% SDS-PAGE gel. Protein was transferred onto a nitrocellulose membrane (Bio-Rad) by protein gel blotting. The membrane was blocked to remove nonspecific binding using 8% milk powder in TBS-T (10 mM Tris-HCl, pH 7.5, 150 mM NaCl, and 0.1% [v/v] Triton X-100). A polyclonal antibody made against a C-terminal peptide of UVR8 (VPDETGLTDGSSKGN) and an anti-GFP monoclonal antibody (632375; Clontech) were used to detect UVR8 and GFP-UVR8, respectively. These proteins appeared as doublets in some protein gel blots, but the banding pattern was not consistent and the reason is unknown. Cytosolic UGPase and nuclear histone H3 were detected using polyclonal antibodies (anti-UGPase AS05086 [AgriSera] and antihistone H3, 07-441 [Upstate]). Antibodies were used at 1:3000 dilution and detected using secondary anti-rabbit or anti-mouse antibodies conjugated to horseradish peroxidase (Promega). To visualize the abundant Rubisco large subunit as a loading control, blots were stained with ponceau S (0.1% [w/v] in 1% [v/v] acetic acid). The data shown are representative of at least three independent experiments.

RNA Extraction and RT-PCR Analysis

Total RNA was extracted from leaf tissue by the RNeasy plant mini kit (Qiagen) according to the manufacturer's instructions. cDNA synthesis and RT-PCR of *HY5* and control *ACTIN2* transcripts were performed as described by Brown et al. (2005). For each transcript, amplification was assayed over a range of cycle numbers to select optimal conditions for visualization of the PCR product and quantification. Transcript levels in different RNA samples were compared using cycle numbers within the linear range of amplification.

Chromatin Immunoprecipitation

Chromatin isolation and chromatin immunoprecipitation were performed using the method of Gendrel et al. (2002) as described by Brown et al. (2005). Immunoprecipitation was performed using either a polyclonal anti-GFP antibody (Invitrogen A-11122) at a dilution of 1/100 or the anti-UVR8 antibody at a dilution of 1/500. The immunoprecipitated DNA was used in PCR reactions to amplify fragments from the *HY5* gene promoter (−331 to +23) or control *ACTIN2* gene as described by Brown et al. (2005).

Subcellular Localization Analysis

Transgenic plants were grown on half-strength MS agar plates for 12 d and given the light treatments described in the figure legends. To visualize nuclei, plants were incubated with 50 μg/mL of DAPI (Invitrogen Molecular Probes) for 15 min. The subcellular localization of GFP and DAPI was visualized by a confocal laser scanning microscope (Zeiss LSM510) under water with a ×40 objective. GFP and DAPI were excited using an argon laser at 488 nm and a UV laser at 395 nm, respectively. GFP emission was collected between 505 and 530 nm to avoid crosstalk with chloroplast autofluorescence. The same microscope settings for GFP and DAPI detection were used before and after UV-B illumination. To measure the relative brightness of nuclear GFP fluorescence shown in Figure 3D, we used the region of interest function of the Zeiss LSM510 as described by Trotman et al. (2007). Relative fluorescence values were recorded for >100 nuclei for each treatment, and means were calculated from three independent experiments. For the measurements of percentage of GFP/DAPI colocalization, each nucleus identified by DAPI fluorescence was examined for GFP fluorescence; if any level of GFP fluorescence was detected, the nucleus was scored as showing colocalization, so the relative intensity of nuclear GFP fluorescence did not influence the measurement. Approximately 20 separate images containing at least 20 cells from six different plants were analyzed for each light treatment, time point, or fluence rate. Colocalization analysis was performed on three independent transgenic lines. The data shown are representative of at least three independent experiments.

Accession Number

The Arabidopsis Genome Initiative locus identifier for *UVR8* is At5g63860.

ACKNOWLEDGMENTS

E.K. was supported by a University of Glasgow Research Studentship. G.I.J. thanks the UK Biotechnology and Biological Sciences Research Council for the support of his research. We thank Robert Sablowski and Clare Lister (John Innes Centre) for seeds of the *35S$_{pro}$:GFP* line, Dan Kliebenstein (University of California, Davis) for *uvr8-1* seeds, Catherine Cloix, Ufo Sutter, Bobby Brown, and John Christie for advice with experimental procedures, and all members of the Jenkins and Christie laboratories for helpful discussions.

Received June 1, 2007; revised July 13, 2007; accepted August 9, 2007; published August 24, 2007.

REFERENCES

A-H-Mackerness, S., John, C.F., Jordan, B., and Thomas, B. (2001). Early signaling components in ultraviolet-B responses: Distinct roles for different reactive oxygen species and nitric oxide. FEBS Lett. **489:** 237–242.

A-H-Mackerness, S., Surplus, S.L., Blake, P., John, C.F., Buchanan-Wollaston, V., Jordan, B.R., and Thomas, B. (1999). Ultraviolet-B-induced stress and changes in gene expression in *Arabidopsis thaliana*: Role of signalling pathways controlled by jasmonic acid, ethylene and reactive oxygen species. Plant Cell Environ. **22:** 1413–1423.

Allan, A.C., and Fluhr, R. (1997). Two distinct sources of elicited reactive oxygen species in tobacco epidermal cells. Plant Cell **9:** 1559–1572.

Ballaré, C.L., Barnes, P.W., and Flint, S.D. (1995). Inhibition of hypocotyl elongation by ultraviolet-B radiation in de-etiolating tomato seedlings.1. The photoreceptor. Physiol. Plant **93:** 584–592.

Barta, C., Kalai, T., Hideg, K., Vass, I., and Hideg, E. (2004). Differences in the ROS-generating efficacy of various ultraviolet wavelengths in detached spinach leaves. Funct. Plant Biol. **31:** 23–28.

Bechtold, N., and Pelletier, G. (1998). *In planta Agrobacterium*-mediated transformation of adult *Arabidopsis thaliana* plants by vacuum infiltration. In *Arabidopsis* Protocols, J.M. Martínez-Zapater and J. Salinas, eds (Totowa, NJ: Humana Press), pp. 259–266.

Boccalandro, H.E., Mazza, C.A., Mazzella, M.A., Casal, J.J., and Ballaré, C.L. (2001). Ultraviolet B radiation enhances a phytochrome-B-mediated photomorphogenic response in Arabidopsis. Plant Physiol. **126:** 780–788.

Bornman, J.F., Reuber, S., Cen, Y.-P., and Weissenböck, G. (1997). Ultraviolet radiation as a stress factor and the role of protective pigments. In Plants and UV-B: Responses to Environmental Change, P.J. Lumsden, ed (Cambridge, UK: Cambridge University Press), pp.157–168.

Brosché, N., and Strid, A. (2003). Molecular events following perception of ultraviolet-B radiation by plants. Physiol. Plant **117:** 1–10.

Brown, B.A., Cloix, C., Jiang, G.H., Kaiserli, E., Herzyk, P., Kliebenstein, D.J., and Jenkins, G.I. (2005). A UV-B-specific signaling component orchestrates plant UV protection. Proc. Natl. Acad. Sci. USA **102:** 18225–18230.

Caldwell, M.M., Björn, L.O., Bornman, J.F., Flint, S.D., Kulandaivelu, G., Teramura, A.H., and Tevini, M. (1998). Effects of increased solar ultraviolet radiation on terrestrial ecosystems. Photochem. Photobiol. **B46:** 40–52.

Caldwell, M.M., Bornman, J.F., Ballaré, C.L., Flint, S.D., and Kulandaivelu, G. (2007). Terrestrial ecosystems, increased solar ultraviolet radiation, and interactions with other climate change factors. Photochem. Photobiol. Sci. **6:** 252–266.

Casati, P., Stapleton, A.E., Blum, J.E., and Walbot, V. (2006). Genome-wide analysis of high-altitude maize and gene knockdown stocks implicates chromatin remodeling proteins in response to UV-B. Plant J. **46:** 613–627.

Casati, P., and Walbot, V. (2004). Rapid transcriptome responses of maize (*Zea mays*) to UV-B in irradiated and shielded tissues. Genome Biol. **5:** R16.

Cho, Y., Yoo, S., and Sheen, J. (2006). Regulatory functions of nuclear hexokinase1 complex in glucose signalling. Cell **127:** 579–589.

Christie, J.M., and Jenkins, G.I. (1996). Distinct UV-B and UV-A/blue light signal transduction pathways induce chalcone synthase gene expression in Arabidopsis cells. Plant Cell **8:** 1555–1567.

Dai, Q.J., Yan, B., Huang, S.B., Liu, X.Z., Peng, S.B., Miranda, M.L.L., Chavez, A.Q., Vergara, B.S., and Olszyk, D.M. (1997). Response of oxidative stress defense systems in rice (*Oryza sativa*) leaves with supplemental UV-B radiation. Physiol. Plant **101:** 301–308.

Dostie, J., Ferraiuolo, M., Pause, A., Adam, S.A., and Sonenberg, N. (2000). A novel shuttling protein, 4E-T, mediates the nuclear import of the mRNA 5′ cap-binding protein eIF4E. EMBO J. **19:** 3142–3156.

Ensminger, P.A. (1993). Control of development in plants and fungi by far-UV radiation. Physiol. Plant **88:** 501–508.

Frohnmeyer, H., and Staiger, D. (2003). Ultraviolet-B radiation-mediated responses in plants. Balancing damage and protection. Plant Physiol. **133:** 1420–1428.

Fuglevand, G., Jackson, J.A., and Jenkins, G.I. (1996). UV-B, UV-A, and blue light signal transduction pathways interact synergistically to regulate chalcone synthase gene expression in Arabidopsis. Plant Cell **8:** 2347–2357.

Gendrel, A.V., Lippman, Z., Yordan, C., Colot, V., and Martienssen, R.A. (2002). Dependence of heterochromatic histone H3 methylation patterns on the *Arabidopsis* gene *DDM1*. Science **297:** 1871–1873.

Hahlbrock, K., and Scheel, D. (1989). Physiology and molecular biology of phenylpropanoid metabolism. Annu. Rev. Plant Physiol. Plant Mol. Biol. **40:** 347–369.

He, Z., Cho, Y., Ma, W., Choi, H.S., Bode, A.M., and Dong, Z. (2005). Regulation of ultraviolet B-induced phosphorylation of histone H3 at serine 10 by Fyn kinase. J. Biol. Chem. **280:** 2446–2454.

Hiltbrunner, A., Tscheuschler, A., Viczián, A., Kunkel, T., Kircher, S., and Schäfer, E. (2006). FHY1 and FHL act together to mediate the nuclear accumulation of the phytochrome A photoreceptor. Plant Cell Physiol. **47:** 1023–1034.

Izaguirre, M.M., Scopel, A.L., Baldwin, I.T., and Ballaré, C.L. (2003). Convergent responses to stress. Solar ultraviolet-B radiation and *Manduca sexta* herbivory elicit overlapping transcriptional responses in field-grown plants of *Nicotiana longiflora*. Plant Physiol. **132:** 1755–1767.

Jansen, M.A.K., Gaba, V., and Greenberg, B.M. (1998). Higher plants and UV-B radiation: Balancing damage, repair and acclimation. Trends Plant Sci. **3:** 131–135.

Jenkins, G.I., and Brown, B.A. (2007). UV-B perception and signal transduction. In Light and Plant Development, G.C. Whitelam and K.J. Halliday, eds (Oxford, UK: Blackwell Publishing), pp.155–182.

Jenkins, G.I., Long, J.C., Wade, H.K., Shenton, M.R., and Bibikova, T.N. (2001). UV and blue light signalling: Pathways regulating chalcone synthase gene expression in *Arabidopsis*. New Phytol. **151:** 121–131.

Kannan, S., and Jaiswal, A.K. (2006). Low and high dose UVB regulation of transcription factor NF-E2-Related Factor 2. Cancer Res. **66:** 8421–8429.

Kim, B.C., Tennessen, D.J., and Last, R.L. (1998). UV-B-induced photomorphogenesis in *Arabidopsis thaliana*. Plant J. **15:** 667–674.

Kircher, S., Kozma-Bognar, L., Kim, L., Adam, E., Karter, K., Schäfer, E., and Nagy, F. (1999). Light quality-dependent nuclear

import of the plant photoreceptors phytochrome A and B. Plant Cell **11:** 1445–1456.

Kliebenstein, D.J., Lim, J.E., Landry, L.G., and Last, R.L. (2002). Arabidopsis *UVR8* regulates ultraviolet-B signal transduction and tolerance and contains sequence similarity to human *Regulator of Chromatin Condensation 1*. Plant Physiol. **130:** 234–243.

Kong, M., Barnes, E.A., Ollendorff, V., and Donoghue, D.J. (2000). Cyclin F regulates the nuclear localization of cyclin B1 through a cyclin-cyclin interaction. EMBO J. **19:** 1378–1388.

Li, J.Y., Ou-lee, T.M., Raba, R., Amundson, R.G., and Last, R.L. (1993). Arabidopsis flavonoid mutants are hypersensitive to UV-B irradiation. Plant Cell **5:** 171–179.

Matsushita, T., Mochizuki, N., and Nagatani, A. (2003). Dimers of the N-terminal domain of phytochrome B are functional in the nucleus. Nature **424:** 571–574.

Oravecz, A., Baumann, A., Máté, Z., Brzezinska, A., Molinier, J., Oakeley, E.J., Ádám, É., Schäfer, E., Nagy, F., and Ulm, R. (2006). CONSTITUTIVELY PHOTOMORPHOGENIC1 is required for the UV-B response in *Arabidopsis*. Plant Cell **18:** 1975–1990.

Paul, N.D., and Gwynn-Jones, D. (2003). Ecological roles of solar UV radiation: Towards an integrated approach. Trends Ecol. Evol. **18:** 48–55.

Shinkle, J.R., Atkins, A.K., Humphrey, E.E., Rodgers, C.W., Wheeler, S.L., and Barnes, P.W. (2004). Growth and morphological responses to different UV wavebands in cucumber (*Cucumis sativum*) and other dicotyledonous seedlings. Physiol. Plant **120:** 240–248.

Shinkle, J.R., Derickson, D.L., and Barnes, P.W. (2005). Comparative photobiology of growth responses to two UV-B wavebands and UV-C in dim-red-light- and white-light-grown cucumber (*Cucumis sativus*) seedlings: Physiological evidence for photoreactivation. Photochem. Photobiol. **81:** 1069–1074.

Stapleton, A.E., and Walbot, V. (1994). Flavonoids can protect maize DNA from the induction of ultraviolet-radiation damage. Plant Physiol. **105:** 881–889.

Stratmann, J. (2003). Ultraviolet-B radiation co-opts defense signaling pathways. Trends Plant Sci. **8:** 526–533.

Trotman, L.C., et al. (2007). Ubiquitination regulates PTEN nuclear import and tumor suppression. Cell **128:** 141–156.

Ulm, R., Baumann, A., Oravecz, A., Mate, Z., Adam, E., Oakeley, E.J., Schäfer, E., and Nagy, F. (2004). Genome-wide analysis of gene expression reveals function of the bZIP transcription factor HY5 in the UV-B response of *Arabidopsis*. Proc. Natl. Acad. Sci. USA **101:** 1397–1402.

Ulm, R., and Nagy, F. (2005). Signalling and gene regulation in response to ultraviolet light. Curr. Opin. Plant Biol. **8:** 477–482.

Wade, H.K., Bibikova, T.N., Valentine, W.J., and Jenkins, G.I. (2001). Interactions within a network of phytochrome, cryptochrome and UV-B phototransduction pathways regulate chalcone synthase gene expression in *Arabidopsis* leaf tissue. Plant J. **25:** 675–685.

Weisshaar, B., and Jenkins, G.I. (1998). Phenylpropanoid biosynthesis and its regulation. Curr. Opin. Plant Biol. **1:** 251–257.

Wen, W., Meinkoth, J.L., Tsien, R.Y., and Taylor, S.S. (1995). Identification of a signal for rapid export of proteins from the nucleus. Cell **82:** 463–473.

Yamaguchi, R., Nakamura, M., Mochizuki, N., Kay, S.A., and Nagatani, A. (1999). Light-dependent translocation of a phytochrome B-GFP fusion protein to the nucleus in transgenic *Arabidopsis*. J. Cell Biol. **145:** 437–445.